J. Pharm. Res. 2024;23(2):89–106

Print ISSN: 0973-7200
Online ISSN: 2454-8405

Journal of Pharmaceutical Research

ORIGINAL ARTICLE

Topical Delivery of Voriconazole Loaded on Lyotropic Liquid Crystal Gel for Management of Fungal Infections

Mohamed A Attia Shafie[1,*], Maha Abdel-Azeem Hassan Mohamed[1], Ahmed Abd-El Zaher Saadi Mohamed[1]

[1] *Department of Pharmaceutics, Faculty of Pharmacy, Assiut University, Assiut, 71526, Egypt*

ARTICLE INFO

Article history:
Received 16-04-2024
Accepted 24-05-2024
Published 06.08.2024

[*] *Corresponding author.*
Mohamed A Attia Shafie
m.attia@aun.edu.eg

https://doi.org/10.18579/jopcr/v23.2.32

ABSTRACT

Topical antifungal therapy is recommended for the treatment of fungal infections of the skin. Due to its benefits, including the ability to direct drugs to the infection site and a lower chance of systemic adverse effects. The nano size and structure of LLC with the skin enhance the permeation and deposition of drugs within deep parts of skin. In this a novel formulation of voriconazole LLC gel was planned. Surfactant, co-surfactant, oil, and water pseudo-ternary phase diagrams were created in order to determine the LLC gel and microemulsion zones. The formulations were evaluated using polarizing microscopy, FT-IR spectroscopy. For each formulation, the polydispersity index, zeta potential, and mean droplet size were determined. The release patterns revealed that the prepared LLC gel provide sustained release profile up to 24 hr. *Ex-vivo* permeation of selected formulations exhibited higher permeability values for voriconazole. The drug skin deposition results from selected formulations showed that, in comparison to other studied formulations, a much larger amount of the drug was deposited in the skin after 24 hours. The confocal pictures appeared that the LLC gel was able to provide fluorescent color to all skin layers. The skin irritation study data of LLC gel formulations could be announced as safe and non- irritant for human skin. The selected formulations underwent a six-month stability testing at room temperature and 4–8 °C. The results showed that the pH, drug content, and viscosity values did not change significantly during this time.

Keywords: Lyotropic liquid crystal; Release and diffusion; Skin permeability; Skin deposition; Pathohistology

INTRODUCTION

Conventional topical options have several limitations and are compromised with regard to patient compliance, safety and efficacy of the therapy. All these subjects demand the need for the development of new carrier systems that could effectively improve skin penetration and reduce the undesirable side effects associated with the drug.

The design of nanomedicines is based on nanosystems, which proficiently control the release of a therapeutic moiety to the affected region at the skin site with localized effect by creating skin reservoirs. Furthermore, nanosized particles and their narrow size distribution may allow an efficient site-specific skin targeting favoring greater drug retention. The entrapment of active moiety in nanocarriers, may provide a base for a new generation of skin delivery of bioactive compounds. Such systems may enable sustained release, resulting in an extended activity or enhanced uptake and the possible reduction in adverse effects [1]. A wide variety of topical agents belonging to different classes of antifungals are available as creams, ointments, gels, lotions, powders, shampoos, and other formulations. Voriconazole is a new broad spectrum second-generation triazole antifungal drug derived from fluconazole. voriconazole was approved by FDA in May 2002. Voriconazole is a powerful antifungal drug that works against all *Candida* species that are resistant to fluconazole. It also works against *Scedosporium, Fusarium*, and *Aspergillus* species that cause infections in the skin, bladder, kidneys, abdomen, and wounds [2].

Muhammad Shah et.al [3] develop chitosan-based voriconazole nanoparticles (NPs) using spray-drying technique. The voriconazole-loaded NPs were investigated for antifungal activity against *Candida albicans* (*C. albicans*). The NPs containing SLS, T80, and PG exhibited the best

KRUPANIDHI COLLEGE OF PHARMACY

penetration and skin retention profile. In addition, the formulation exhibited a potential antifungal effect against *C. albicans*.

In a study by Liu et al. (2023), a liposome containing voriconazole showed a greater capacity for binding to the chitin of the fungal cell wall of *C. albicans*. Furthermore, the in vivo study improved the delivery efficacy of voriconazole [4].SehHyon Song et.al developed topical preparations of voriconazole (VRC) for the treatment of mycotic infections of the skin, a nanostructured lipid carrier-based hydrogel (NLC-gel) formulation was developed. The NLC-gel markes greater accumulation of VRC in deeper skin layers as compared with the reference formulation [5].

Prasanna Raju Ya et.al developed microemulsion-based hydrogel for voriconazole. Oleic acid and isopropyl myristate as lipid phases; tween 20: tween 80 as surfactants and PEG600 as cosurfactant voriconazole microemulsion based hydrogel systems had been depicted significant antifungal potentials in comparison with standard drug [6].

Lyotropic liquid crystals (LLC) are thermodynamically stable ordered structures that occur in mixtures of surfactants, co-surfactants and oil with one or several solvents usually water. The nano size of these compounds improves the skin permeation of drugs. The structure resemblance of lyotropic liquid crystals with skin membrane (bilayer) enhances the skin retention of drugs.

The aim of this research article is to formulate and characterize lyotropic liquid crystalline gel for topical delivery of voriconazole for treatment of skin fungal infections.

EXPERIMENT

Materials and Methods

Voriconazole was kindly provided by Global Napi Pharmaceuticals, (Giza, Egypt);Sesame oil and Soyabean oil were obtained from ISO CHEM Co. (Cairo, Egypt); Cremophor RH 40® (Polyoxy 40 hydrogenated castor oil) were obtained from NEROL Co. (Cairo, Egypt); Polyethylene glycol 600 (PEG 600) was obtained from MORGAN chemicals (Cairo, Egypt); Glycerin was obtained from El Gomhouria Co. (Assiut, Egypt); Sodium orthophosphate and di-sodium orthophosphate were obtained from El Nasr pharmaceutical chemicals Co., Egypt ; Methanol (99%) and Isopropyl alcohol (99%) were obtained from El Nasr pharmaceutical chemicals Co., Egypt. All other chemicals used of analytical grade and used without further purification.

Construction of calibration curves of voriconazole

The calibration curve was constructed by accurately weighing 10 mg of voriconazole and dissolving them in 100 ml of phosphate buffer: methanol mixture (95: 5 % v/v), isopropyl alcohol and methanol to obtain a 100 μg/mL stock solution. Further dilutions were made to obtain different concentrations corresponding to 5, 10, 15, 20, 25, 30, 35, and 40 μg/mL of the drug. The absorbance of these solutions was determined spectrophotometrically at 256 nmusing the same solvent medium as a blank. Each experiment was carried out in triplicate and the average absorbance was plotted against the concentrations (μg/mL) to construct the standard calibration curve.

Construction of pseudo-ternary diagrams

The pseudo-ternary phase diagrams of oil, surfactant, co-surfactant and water were constructed using water titration method [7]. Heating (at 70 °C) was required to facilitate mixing. A non-ionic surfactant (cremophor RH 40) was mixed with glycerin or PEG-600 as co-surfactant to obtain surfactant and co-surfactant mixture (S/Co mix) at a weight ratio of 1:1, 2:1 and 3:1. Each S/Co mix were then mixed with oil at 70 °C. For each phase diagram, the ratio of oil to the S/Co mix was varied as 1:9, 2:8, 3:7, 4:6, 5:5, 6:4, 7:3, 8:2 and 9:1 (w/w). The resulting mixtures were subsequently warmed to 70 °C using hot plate magnetic stirrer and titrated with previously warm distilled water (70 °C) with continuous stirring (500 rpm). The samples cooled at room temperature and left to equilibrate overnight, the samples were checked visually for transparency and determined as clear and transparent microemulsions or white turbid simple emulsions and clear highly viscus gel. No attempt was made to distinguish between oil-in-water, water-in-oil microemulsions. The samples were marked as points in the phase diagram.

The sample ratios that have resulted in the formation of clear liquid microemulsions and gels were plotted as points on the pseudo-ternary phase diagrams using CHEMIX School program version 5© (Arne Standnes, Bergen, Norway). Visually clear samples of high viscosity were additionally checked through the cross polarizer for the presence of liquid crystalline phase. No attempts were made to completely identify the other regions of pseudo-ternary phase diagram in detail.

Determination of drug solubility in LLCs gel components

To ensure the capacity of LLCs gel to dissolve voriconazole. Solubility of voriconazole in different components of LLCs gel were determined by shaking flask method. An excess amount of drug was added to each glass vial containing 2 grams of each vehicle (sesame oil, soyabean oil, glycerin, polyethylene glycol 600, cremophor RH 40). The obtained mixtures were mixed for 5 minutes using vortex mixer to facilitate drug mixing, the mixtures were kept at a temperature of 37$\pm$0.5 °C in temperature controlled shaking water bath at 100 rpm for 72 hr. Samples were centrifuged at 10000 rpm for 15 min to remove undissolved drug, the supernatant solution was filtered through a 0.45 μm membrane filter. The concentration of voriconazole in the supernatants was determined using a UV-vis spectrophotometer at λ_{max} of 256 nm [8]. All experiments were conducted in triplicates

and voriconazole solubility (mg/mL) in each vehicle was recorded as mean value ± SD.

Preparation of voriconazole lyotropic liquid crystals gels

The composition of twelve formulations (F1-F12) were chosen from the gel region of pseudo-ternary diagram as expressed in Table 1. From the pseudo-ternary diagram, the selected formulation was chosen following the criteria of having the lowest concentration of surfactants, the highest proportion of the aqueous phase, and having gel consistency. It was reported that specific hydration of the stratum corneum affected the skin permeability[9]. The oil was added to the S/Cos mix and stirred gently until complete mixing at 70 °C. Then, 0.5% w/w voriconazole was added with stirring until it had been completely dissolved. Then, a defined weight of distilled water was added drop wise with gentle stirring, the formulations allowed to cool to room temperature. The prepared LLCs gel formulations were finally stored in closed glass vials.

Preparation of voriconazole carbopol gel

Carbopol gel containing voriconazole was prepared for comparison with LLC gel. Voriconazole (0.5 % w/w) was dispersed in distilled water, then 1 % w/w carbopol 934 was added to the dispersion and stirred till homogenous mixture was obtained. Triethanol amine (8-10 % w/w) finally added to form gel[10].

Characterization of the LLCs gel formulations

- **Polarized light microscope**

Polarized light microscope was used to establish the liquid crystalline structures. The structure of the unloaded and drug-loaded LLC samples was examined with a polarized light microscope. LLC gel were spread over glass slide then a cover glass was slowly placed on the glass slide to avoid entrapment of air bubbles. Samples were analyzed at 10X and 20X magnification using a polarized optical microscope and images were taken with a digital camera.

- **X-ray diffraction**

The existence of regularly organized structures was demonstrated by the X-ray diffraction measurements. The X-ray phase studies were performed on a Bruker D8 Advance diffractometer, using CuKa1 radiation (40 kV, 40 mA) monochromated using a Johansson curved monochromator (l =1.5406 A).

- **Fourier transform-infrared spectroscopy (FT-IR)**

Fourier transform-infrared spectroscopy (FT-IR) technique was used to detect if there is interaction between voriconazole and any components of LLCs gel formulations. Potassium bromide (KBr) discs were prepared by mixing samples with finely powdered potassium bromide into a mortar and then condensed in a 13-mm die at a pressure of 8-9 tons / square inch for 5 minutes. The discs were scanned from 4000 to 400 cm^{-1}.

Table 1: Compositions of selected viscous LLC gel formulations

Formula Code	Surfactant (S)	Co-surfactant (Co)	S:Co mix	Oil	(S:Co mix): oil : water % w/w
F1	Cremophor RH 40	Glycerin	1:1	Sesame	61.54 : 15.38 : 23.08
F2	Cremophor RH 40	Glycerin	1:1	Soyabean	53.84 : 23.07 : 23.09
F3	Cremophor RH 40	Glycerin	2:1	Sesame	56.25 : 6.25 : 37.5
F4	Cremophor RH 40	Glycerin	2:1	Soyabean	52.94 : 5.88 : 41.18
F5	Cremophor RH 40	Glycerin	3:1	Sesame	52.94 : 5.88 : 41.18
F6	Cremophor RH 40	Glycerin	3:1	Sesame	50 : 12.5 : 37.5
F7	Cremophor RH 40	Glycerin	3:1	Sesame	46.66 : 20 : 33.34
F8	Cremophor RH 40	Glycerin	3:1	Soyabean	47.05 : 11.76 : 41.19
F9	Cremophor RH 40	PEG 600	2:1	Sesame	50 : 12.50 : 37.50
F10	Cremophor RH 40	PEG 600	2:1	Soyabean	50 : 12.50 : 37.50
F11	Cremophor RH 40	PEG 600	3:1	Sesame	47.37 : 5.26 : 47.37
F12	Cremophor RH 40	PEG 600	3:1	Soyabean	47.37 : 5.26 : 47.37

- **Determination of mean droplet size, polydispersity index and zeta potential**

The mean droplet size, polydispersity index and zeta potential were determined by dynamic light scattering (DLS) technique using Malvern Zetasizer Nano Series ZS (Malvern instruments, UK), where 1 gram of LLCs gel formulation was dispersed in 9 gram of distilled water using mechanical stirrer. Samples were placed in square glass cuvettes then the droplet size and zeta potential were measured. All

measurements were carried out in triplicate and recorded as mean value ± SD.

- **Determination of LLCs gel pH**

The pH of all formulations was determined by using calibrated pH meter. One gram of LLC gel formulation was dispersed in 9-gram distilled water by mechanical stirrer (500 rpm) and measurements were carried out at room temperature. The device was calibrated with the standard buffer solutions of pH 4.0 and 7.0 before measuring the pH value.

- **Determination of drug content**

Voriconazole content in LLC gel formulations was determined by dissolving 0.250 g of LLC gel in Isopropyl alcohol by vortex then sonication. Absorbance was measured after suitable dilution at 256 nm by UV-spectrophotometer and % drug content was calculated and compared with theoretical amount in 250 mg of LLC gel.

$$Drug\ content\ (\%) = \frac{Actual\ amount\ of\ drug\ in\ gel}{Theoretical\ amount\ of\ drug\ in\ gel} \times 100$$

- **Determination of rheological behavior**

Rheological behavior of the drug loaded LLC gel formulations was determined using Brookfield rheometer. The viscometer was fitted with T-F spindle 96 and the viscosity was determined at different shear rates from 10 to 80 rpm. The samples were measured at room temperature and all measurements were performed in triplicates.

- **Spreadability test**

The Spreadability of the prepared LLCs gel formulations was determined using parallel plate method[11]. Briefly, 0.5 g gel formulation was pressed between two glass plates for 1 minute[12]. The weight of the upper glass plate was 44.89 g. The average diameter obtained from each formulation was measured. The results are the average of three determinations. Spreadability was determined by the following equation[13]:

$$S = ML/T$$

Where: M = weight of the upper glass plate (g), L = Diameter in (cm) and T = Time taken in (sec).

- ***In-vitro* voriconazole release study**

In-vitro drug release from selected voriconazole LLCs gel formulations were studied using dialysis tube method. The cellulose membrane (molecular weight cut-off 12,000–14,000 Da) previously soaked overnight in phosphate buffer solution (pH 7.4) was tied to one end of a specially designed glass cylinder (open at both ends) having inner diameter of 2.4cm. In the donor compartment, one gram of selected LLCs gel formulation containing 5 mg voriconazole was spread over previously soaked cellulose membrane fitted at the lower end of glass tube. The cylinder was suspended in a beaker (receptor chamber) containing 100 mL phosphate buffer (pH 7.4) and maintained at 37 ± 0.5 °C. The solubility of voriconazole in PBS (pH 7.4) solution was determined as approximately 0.634 mg/mL. This equilibrium solubility guarantees the sink conditions for voriconazole.

The procedure was carried out in a thermostatically controlled shaking water bath operating at 50 rpm and at a temperature of 37±0.5 °C. At defined time intervals, 5 mL of the release medium was withdrawn from the receptor compartment and replaced with equal volume of fresh release medium to preserve sink conditions. The samples were analyzed using UV-spectrophotometer at λ_{max} 256 nm. The release experiments were performed in triplicates and the mean % of cumulative drug release ± SD were calculated. The obtained results were plotted as a cumulative drug release percentage (CDR %) versus time.

- **Mechanisms and kinetics of *in-vitro* drug release**

In order to determine the mechanism of drug release from gel formulations, various kinetic models were used. *In-vitro* release data of LLC gel formulations were fitted to different models (zero, first and Higuchi diffusion model).

Ex-vivo skin permeability study

The assessment of percutaneous absorption is one of the main steps in the evaluation of any dermal or transdermal drug delivery system. The skin permeation experiments are known for their value for studying the rate and mechanisms of the percutaneous absorption of drugs. The *in-vitro* drug permeation through rat skin was used to measure drug permeation. The Wister rat skin model has been used extensively in the view of the fact that its stratum corneum thickness as well as water permeability are similar to that of human skin[14].

The formulations with good release profile (F3, F4, F5, F11 and F12) were selected for *ex-vivo* permeation testing. Carbopol gel containing 0.5% w/w voriconazole was used as control.

- **Preparation of rat skin**

The *in-vitro* skin permeation studies of different gel formulations were carried out using full thickness rat skin. The experimental procedures were performed in accordance with the institutional Animal Ethical Committee of Faculty of medicine, Assiut university (Approval no: 17101917). Male Wistar albino rats (200-250 g) were purchased from the animal house of the faculty of veterinary medicine, Assiut University. Rates were anesthetized using intraperitoneal injection of ketamine (50 mg/Kg of body weight) and midazolam (5 mg/Kg of body weight). Hair was carefully

removed using an animal hair clipper 24 hr before the experiment. The rats were sacrificed, and their dorsal skin was separated from the underlying connective tissue with scalpel. Dermis part of the skin was wiped three times with a wet cotton swab soaked in isopropanol to remove any adhering fat material. Then, the skin was kept in normal saline solution for two hours. The cleaned skin was washed with distilled water, wrapped in aluminum foil, and stored in a deep freezer at – 20°C and used within two weeks.

- **Skin permeation study**

The *in-vitro* permeation studies were carried out in Hanson vertical diffusion Cell system with a diffusion area of 1.767 cm^2 and capacity of 7 mL for the receptor medium, PBS pH 7.4. The Franz Cell system was maintained at a constant temperature of 37.5 $\pm$1 °C, while the receptor medium was stirred constantly at 300 rpm during the experiments.

The skin was mounted between the donor and receptor compartments of the diffusion cell with the SC facing upward (donor compartments). 0.25 gram of voriconazole LLC gel formulation (containing to 1.25 mg voriconazole) was placed on the donor compartment. At appropriate time intervals up to 24 hr, samples of 1 mL from the receptor compartment were withdrawn and replaced by an equal volume of fresh medium to keep a constant release medium in the receptor compartment. The samples from the receptor compartment were filtered by 0.22 μm disc filter and assayed using UV spectrophotometer at λ_{max} 256 nm. The experiments were repeated in triplicate. Cumulative amount of voriconazole permeated through the skin ($\mu g/cm^2$) was plotted as a function of time.

The permeation rate of drug at steady state (Flux, Jss, $\mu g\ cm^{-2}h^{-1}$) was calculated from the slope of the plots of cumulative amount of drug permeated vs. time in steady state conditions. Apparent permeability coefficient (Papp, cm/h) was calculated by dividing the flux with initial concentration of drug in the donor compartment (Papp = Jss/Co)[15].

- **Skin deposition study**

At the end of the drug permeation studies, the skin was used to determine the amount of drug deposited in rat skin. For this purpose, Skin was removed where effective permeation area (1.76 cm^2) of skin was cut, washed with distilled water and dried between two filter paper, the skin was cut to small pieces and place into a glass vial containing 5 mL methanol as a drug extraction solvent for 24 hr, after sonication for 30 min, The extract was subsequently filtered through a 0.22 μm filter and was analyzed for drug content by UV spectrophotometer at λ_{max} 256 nm.

Skin penetration behavior of voriconazole from LLC gel

To visualize the penetration behavior of voriconazole into skin layers which was loaded into LLC gel formulations and to predict drug distribution in the skin. Confocal laser scanning microscope (CLSM) images of the skin samples treated with LLCs gel were analyzed. In this respect, the fluorescent marker namely, rhodamine B (log P: 1.95) which have similar lipophilic features with voriconazole was used as the substitute of drug. F3 and F12 labeled with $1.25x10^{-3}$ % (w/w) fluorescent marker were applied to rat skin for 24 hr under the same *in-vitro* skin penetration study conditions. After which the skin was removed from the diffusion cell, rinsed with distilled water and then the surface of the skin was wiped gently. The separated dorsal skin was fixed in paraformaldehyde (4 % w/v) for 30 min. Then, they were washed and dehydrated by serial dilutions of alcohol. Paraffin bees wax tissue blocks were prepared by slide microtome. The obtained tissue sections were collected on glass slides, deparaffinized and examined under confocal laser microscope. The analysis was carried out using laser scanning confocal microscopy operating at excited wavelength of 552 nm and emission wavelength of 580 nm for Rhodamine B probe. The mean fluorescence intensity of each image was analyzed by Image J software[16].

Skin irritation study

The skin irritation test was performed according to the methods of Draize et al. with slight modifications. Wistar albino rats were clipped free of hair 1 day before the experiment. The animals were divided into four groups, Group I served as the control; group II and group III received F3 and F12, respectively; and group IV received a 0.8% w/v aqueous solution of formalin as a standard irritant. Animals were examined for signs of irritation after application. Finally, the skin reactions were evaluated and graded in accordance with the following Draize method (see Table 2). The experimental procedures were performed in accordance with the institutional Animal Ethical Committee of Faculty of medicine, Assiut university (Approval no: 17101917).

Table 2: Skin irritation score values

	Erythema score		Edema formation score
0	No erythema	0	No edema
1	Very slight erythema (light pink discoloration of skin)	1	Very slight edema
2	Moderate to severe erythema (dark pink)	2	Slight edema
3	Well-defined erythema (light red)	3	Moderate edema
4	Severe erythema (dark red)	4	Severe edema

In-vitro antifungal activity

The antifungal activity for the selected formulations (F3, F12, corresponding blank formulations and carbopol gel containing 0.5 % w/w voriconazole as control) were investigated using agar diffusion method. Different species and strains of fungi including *Candida albicans* (AUMC NO.10189), *Aspergillus flavus* (AUMC NO.11618) and *Aspergillus niger* (AUMC NO.11615) were involved. The medium for antifungal activity used was Sabouraud dextrose agar. The media were poured aseptically in glass petri plate and kept till the solidification. The fungal species were inoculated onto agar surface by streaking. A single well was made in each agar plate using a sterile cork borer and filled with an accurately weighed 0.200 gm of each formulation (F3, F12, F3 plain, F12 Plain and carbopol gel containing voriconazole as control). The plates were incubated at 37± 1ºC for 2 days, and then they were examined for the inhibition zone diameter which is indication of antifungal activity. The diameter of zones, including the diameter of the well, was recorded.

In-vivo antifungal study

Twenty-one male Wistar albino rats (200-250 g) were purchased from the animal house of the faculty of veterinary medicine (Assiut University, Egypt) Three rats were housed in each cage with access to standard rat chow pellets and water. The animals were maintained in a 12-hour light/dark cycle in a temperature and humidity-controlled room (25 ± 2 and 60±5 relative humidity). They were housed for acclimatization, one week before starting the experiment. The experimental procedures were performed in accordance with the institutional Animal Ethical Committee of Faculty of medicine, Assiut university (Approval no: 17101917), and adheres to the guide for the care and use of laboratory animals, 8th edition, National Academic press, Washington, DC[17].

- **Preparation of the fungal strain**

To induce the infection, a working culture of *Candida albicans* (AUMC NO.10189) grown for 48hs on Sabouraud dextrose agar. The cells were then collected, washed and suspended in sterile saline to a final concentration of 1×10^7 colony forming units/ml (cfu/ml)[18].

- **Induction of superficial fungal infection**

Hair from the back of the albino rats were removed with the help of hair-removing cream. Sandpaper was gently rubbed on the hairless skin to cause abrasion so that fungal infection can be induced. This abraded skin area was properly disinfected with ethanol before applying inoculum. Sterile cotton impregnated with *Candida albicans* suspension (in the strength of 1×10^7 cfu per mL) was applied on abraded and disinfected skin and kept intact with adhesive tape. Flaring of fungal skin infection was observed for 7 days after induction[19,20]. For confirmation of topical fungal infection induction, the infected skin sample was obtained with a scalpel's help and shifted to a growth medium (Sabouraud dextrose broth). After incubation for one day at 37 °C, the samples were examined under light microscope for Presence of *Candida* infection[21].

- **Treatment of fungal infection**

Treatment began after 7 days of induction of infection and continued for 7 days. Rats were classified in to seven groups (3 rats in each group) according to treatment plan in Table 3. Assessment of topical fungal infection was done by checking sign of more erythema, edema, scales, and cracking at infection site on animal body. The treatment was given once daily for a period of one week. The animals were clinically evaluated for a week in days 1, 3, 5 and 7 of treatment period.

Table 3: *In-vivo* study animal groups

Animal group	Treatment plan
Group 1	Without induction of skin fungal infection (-ve control).
Group 2	Skin fungal infection treated with F12 formulation.
Group 3	Skin fungal infection treated with F3 formulation.
Group 4	Skin fungal infection treated with F12 plain.
Group 5	Skin fungal infection treated with F3 plain.
Group 6	Skin fungal infection treated with voriconazole carbopol gel.
Group 7	Skin fungal infection without treatment (+ve control).

Stability study

Based on results of previous studies, gel formulations of F3 and F12 were stored in well-stoppered glass vials for 6 months at 4°C and room temperature. The stored samples were checked for optical clarity and phase separation by visual inspection and measurement of pH, Viscosity, and voriconazole content at 0-,1,2, 3 and 6-month storage.

Statistical analysis

Statistical analyses were carried out using Graph Pad Prism software version 5. One-way analysis of variance (ANOVA) with newman-keuls post-hoc test was used to analyze the difference between experimental groups. A probability of less than 0.05 ($P< 0.05$) was considered statistically significant. All experiments were conducted in triplicates and presented as means ± SD.

RESULTS AND DISCUSSIONS

Calibration curve of voriconazole in different solvents

The drug calibration curve of voriconazole in each 0f phosphate Buffer (pH 7.4); isopropylalcohol and methanol was found to obey Beer's Lambert law within the concentration range 5 – 40 μg/mL as shown in Figure 1. The obtained line was analyzed by linear regression. The reciprocal value of the slope represented the procedural constant.

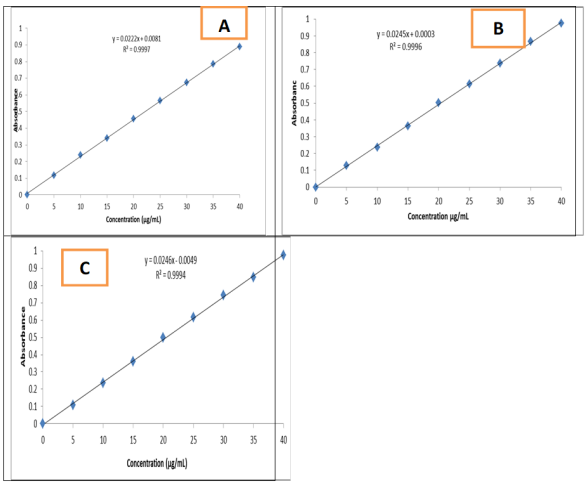

Fig. 1: Standard calibration curve of voriconazole at 256 nm. in A: Posphate buffer (pH 7.4), B: Isopropyl alcohol, C: Methanol

Construction of pseudo-ternary phase diagrams

From the pseudo-ternary phase diagrams obtained, it was evident that, the size of the microemulsion region within the pseudo-ternary phase diagrams expanded with the increment of the surfactant concentration within the S/Co blend, from 1:1 to 2:1 and from 2:1 to 3:1. This increment is for the most part due to the interfacial tension's progressive lowering caused by an increment in surfactant concentration. Comparative to the microemulsion region, the gel region of S/Co blend 3:1 was bigger than that of S/Co blend 2:1, showing the marked impact of the surfactant/co-surfactant (S/Co) weight proportion on the gel phase properties (size and position within the pseudo-ternary phase diagram).

Determination of drug solubility in LLCs gel components

To develop microemulsion formulations for topical delivery of poorly water soluble voricinazole, the optimum oil, surfactant and co-surfactant have to be chosen to confirm the capacity of prepared LLCs gel formulations to solubilize the added amount of voriconazole (0.5 % w/w). The solubility of voriconazole within the different oils, surfactants and co-surfactants are shown in Table 4. The solubility of voriconazole was higher in polyethylene glycol 600 (81.84 mg/ml) and chremophor RH40 (49.68 mg/ml). There were no critical contrasts within the solubility of voriconazole in both sesame oil and soya bean oil. The solubility data demonstrated that the addition of cremophore RH40 and PG to oil led to a different change in drug solubility. The high solubility of voriconazole in surfactant and co-surfactant was advantage to increase its solubility in microemulsions.

Table 4: Solubility of voriconazole in different components of LLCs gel formulations

Vehicle	Solubility (mg/ml)
Sesame oil	7.37 ± 0.14
Soya bean oil	8.24 ± 0.67
Cremophor RH 40	49.68 ± 2.22
Glycerin	4.52 ± 0.30
PEG 600	81.84 ± 3.44

Characterization of the selected LLCs gel formulations

- **Polarized light microscope**

The polarized light micrographs (Figure 2) suggested that the formulations F5;F6 and F7 which have streaks texture (Maltes crosses and ribbon like structures) identified as lamellar LLC[11], while the formulations (F1,F2,F3,F4,F8,F9,F10,F11 and F12) appear as black background identified as cubic LLC[22].

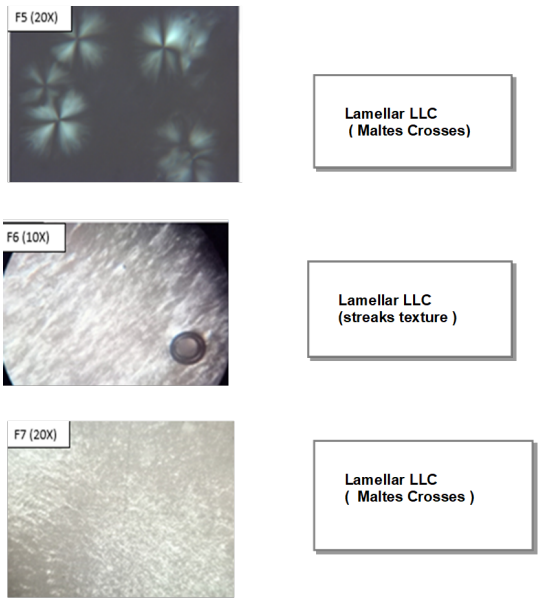

Fig. 2: Textures of liquid crystal samples: Lamellar liquid **crystal F5, F6, and F7**

- **Fourier transform-infrared spectroscopy (FT-IR)**

FT-IR was carried out to examine the compatibility between voriconazole and other LLCs components. Voriconazole FT-IR spectrum (Figure 3) showed OH stretching at 3250–3050 cm^{-1}, aromatic C-H stretching at 3119 cm^{-1}, aliphatic C-H stretching at 2994-2940 cm^{-1}, and C-N stretching at 1507– 1450 cm^{-1}, and C-F stretching at 1586–1473 cm^{-1}, respectively. The given results are in accord with those recorded by khare et al [23]. The spectrum of pure cremophor RH 40 showed the absorption band of the OH group, which was expressed as a broad band at 3436 cm^{-1}. The aliphatic C-H bond was seen as a biforked band with two apices at 2925 and 2858 cm^{-1}. The peak carbonyl group of the ester was found at 1734 cm^{-1}. The ether C–O–C stretching was manifested as a strong broad band at 1111 cm^{-1} [24].

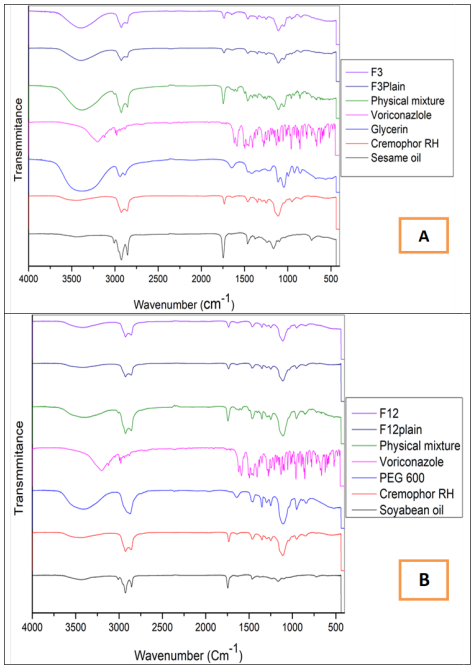

Fig. 3: Stacked IR spectra of F3, F3 plain (A), of F12, F12 plain (B)

The spectrum of soyabean oil and sesame oil showed the absorption band of the OH group, which was expressed as a broad band at 3436 cm^{-1}. The aliphatic C-H bond was seen as a biforked band with two apices at 2925 and 2858 cm^{-1}. The peak carbonyl group of the ester was found at 1746 cm^{-1} [25,26].

The main characteristic peaks of glycerin were observed at 3385 cm^{-1} (OH stretching) and 2886 cm^{-1} (C-H stretching) [27], while main characteristic peaks of PEG 600 observed at 3416 cm^{-1} (OH stretching) and 2876 cm^{-1} (C-H stretching) [28]. It was observed that there was no remarkable change in the peaks of pure drug and LLCs components. Hence, no specific interaction was observed between the drug and the components used in the formulations.

Determination of mean droplet size, polydispersity index and zeta potential

Lyotropic liquid crystals droplet size significantly affects permeation of drug into deeper layers of skin, where small droplet size makes it an excellent carrier for promoting drug percutaneous uptake as the number of droplets that can interact on a fixed area of SC will increase when the particle size decreases.

Table 5 shows the mean droplet size, PDI, zeta potential of the selected LLCs gel formulations. All formulations possess small droplet size in the nano range (below 50 nm), except F2 and F7 (63.27 and 66.9 nm, respectively). The small size was expected due to the presence of co-surfactant molecules and the surfactant, which reduces interfacial tension and thus decreases the radius of droplets [29]. Formulations F2 and F7 showed a significantly larger mean droplet size compared to other formulations ($P < 0.05$). This could be attributed to their higher oil concentration compared to other formulations. Marco et al., reported that, there are linear relationship between oil content and droplet size of the prepared microemulsions [30].

Table 5: Mean droplet size, PDI and zeta potential values of LLC gel formulations

Formulation number	Mean droplet size (nm)	PDI	Zeta potential (mv)
F1	38.5± 0.09	0.098	-8.1 ± 0.33
F2	63.27± 2.90	0.166	-10.4 ± 1.95
F3	24.54± 0.21	0.204	-13.7 ± 1.33
F4	24.4± 1.00	0.220	-14.7 ± 1.23
F5	23.07 ± 0.91	0.141	-16.2 ± 0.72
F6	30.47 ± 1.19	0.159	-10.5 ± 1.89
F7	66.92 ± 1.55	0.240	-7.8 ± 0.14
F8	32.77 ± 0.98	0.194	-10.2 ± 0.57
F9	33.63 ± 0.81	0.126	-5.5 ± 0.40
F10	33.57 ± 0.19	0.172	-10.2 ± 1.05
F11	24.27± 0.30	0.224	-5.6 ± 0.59
F12	23.623 ± 0.07	0.221	-7.5 ± 0.11

The influence of the different ratios of surfactant (Cremophor RH40) to co-surfactant (glycerin or PEG 600) on the droplet the ratio of surfactant to co-surfactant increased from 1:1 to 2:1 (when use glycerin as co-surfactant) and from 2:1 to 3:1 (when use PEG 600) as co-surfactant. This may be attributed to the increased proportion of surfactant which further produce more size reduction [30,31].

PDI results showed that all of the formulations had droplets in the nano range. The homogeneity of droplet size within the formulation is shown by the PDI, which is the ratio of standard deviation to mean droplet size. The

uniformity of the droplet size in the formulation decreases with increasing PDI[32]. PDIs value ranged from 0.098 to 0.240 which shows the narrow distribution of droplet size.

Also, Zeta potential of the formulations was measured for determination of droplet charge and/or electrostatic repulsion. The physical stability of any dispersed systems said to increase with the increase in the electrostatic repulsion energy, which is directly proportional to the particle surface charge and the thickness of the diffusion layer[33]. Due to the presence of a non-ionic surfactant, whose diffusive border has an almost neutral charge and supports the stability of the microemulsion, zeta potential values ranged from -5.5 ± 0.40 to -16.2 ± 0.72. The stability of the LLCs gel system is indicated by a negative zeta potential. According to this finding, all formulations contain sufficient charge and mobility to reduce droplet aggregation[34]. Uniformity of the droplet size in the formulation decreases with increasing PDI[32], PDIs value ranged from 0.098 to 0.240 which shows the narrow distribution of droplet size.

PH Determination of LLCs gel

Table 6 shows pH values of all selected LLCs gel formulations. Since the pH of therapeutic substances applied topically from 5.5 to 6.5, the pH values of the prepared LLC gel could be counted in the tolerable pH range[35].

Table 6: Mean pH values ± SD of LLC formulations

Formulation	Mean pH values ± SD	Formulation	Mean pH values ± SD
F1	6.138 ± 0.003	F7	6.37 ± 0.083
F2	6.193 ± 0.042	F8	5.94 ± 0.092
F3	6.353 ± 0.04	F9	5.72 ± 0.069
F4	5.905 ± 0.045	F10	5.65 ± 0.019
F5	6.15 ± 0.071	F11	5.78 ± 0.021
F6	6.28 ± 0.004	F12	5.86 ± 0.049

Determination of drug content

Good uniformity of drug content among the prepared gel formulations were observed within range from 96.80 ± 1.55 to 102.3 ± 1.26 % w/w (Table 7). These results indicated that the process employed to prepare gels in this study was capable of producing gels with uniform drug content and minimal content variability. Also, drug contents of all formulations were found within limit (90-110 % w/w).

Determination of rheological behavior

The rheological status of a semisolid drug carrier system is a very important physical parameter. All the LLC gel formulations (Figure 4) exhibited a shear thinning flow (pseudo plastic flow) as the viscosity decreased with increasing the shear rate. This result was in agreement with the findings of Savic et al.[36], and Qian et al.[37],who found that the rheological behavior of liquid crystalline gel phases was plastic or pseudoplastic flow behavior, a property desirable for viscous liquid dispersions or semisolids. All the selected LLCs gel formulations have suitable viscosity for topical application. Formation of LLC ordered structures is responsible for the increased viscosity of the systems[11]. Rheological profile of the prepared gel formulations revealed that the formulations with higher surfactant: co-surfactant ratio were more viscous than formulations with lower surfactant: cosurfactant ratio as the following order (3:1 > 2:1> 1:1), this may be attributed to increased concentration of surfactant (Cremophor RH40). It is also observed that gel formulations with glycerin cosurfactant have higher viscosity than formulations with PEG 600 as cosurfactant.

Table 7: Drug content (% w/w) of different LLC formulations

Formulation	Drug content (% w/w)	Formulation	Drug content (% w/w)
F1	99.24 ± 0.63	F7	96.80 ± 1.55
F2	98.58 ± 2.3	F8	97.69 ± 1.57
F3	97.69 ± 0.31	F9	102.3 ± 1.26
F4	101.4 ± 0.94	F10	97.69 ± 3.34
F5	98.13 ± 0.94	F11	98.80 ± 1.89
F6	98.80 ± 1.26	F12	99.91 ± 0.94

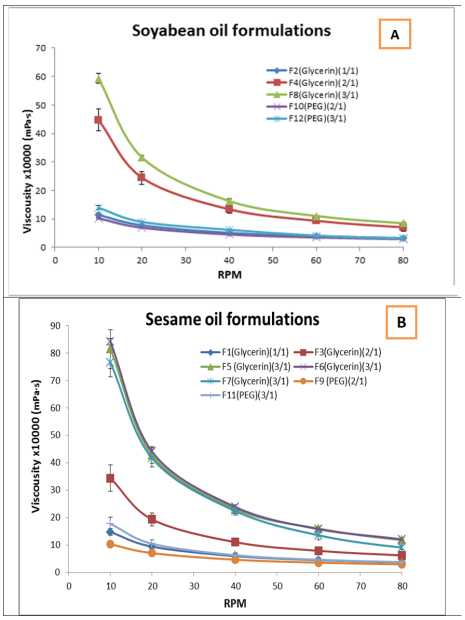

Fig. 4: Rheological behavior of Lyotropic Liquid Crystal formulations based on A. Soyabean Oil, B. Sesame Oil

Spreadability test

Spreadability is the term expressed to denote the extent of area to which the gel readily spreads on application to the skin. The spreadability of topical preparations is an important criterion for standardized and simple application on the skin. The efficacy of the gel or the bio-availability efficiency of the formulation depends on the spreadability value. The higher the value of the gel spreadability, the higher is the absorption area and the higher is the bio-available efficiency of the formulation.

Spreadability test was carried out for all LLCs gel formulations. The results (Table 8) showed that for all formulations, the increase in gel viscosity resulted in to lower spreadability values. These findings were in agreement with Kishor et al.[12]who reported that, the increase in viscosity of gel formulations resulted in poor spreadability values. From the Table 8, it was observed that, formulations F1, F2, F9, F10, F11 and F12 gives higher spreadability values than other formulations, these results may be due to lower viscosity values of these formulations.

Table 8: Spreadability values (g.cm/sec) for LLC formulations

Formulation	Spreadability (g.cm/sec)	Formulation	Spreadability (g.cm/sec)
F1	2.8 ± 0.05	F7	1.60 ± 0.07
F2	2.78 ± 0.03	F8	1.41 ± 0.11
F3	1.90 ± 0.05	F9	2.5 ± 0.15
F4	1.90 ± 0.07	F10	2.50 ± 0.08
F5	1.53 ± 0.05	F11	2.09 ± 0.02
F6	1.45 ± 0.06	F12	2.05 ± 0.04

In-vitro voriconazole release study

The release patterns (Figure 5) revealed that, drug release rate from various LLC gel formulations was significantly slower than that from carbopol gel containing 0.5 % w/w voriconazole (P< 0.001), this ensure that LLCs gel formulations provide sustained release effect. Carbopol gel showed more than 50 % release of voriconazole within first 4 hr whereas the LLCs gel formulations released less than 20 % of voriconazole within first 4 hr. Voriconazole release was successfully prolonged due to the previously discussed high viscosities of LLC gel formulations. Results demonstrated that all LLCs gel formulations caused a sustained drug release up to 24 hours. Makai et al.[38] reported the ability of LLCs systems to prolong the release of water soluble and water insoluble drugs. Also, sustained release profile of gel formulations may be attributed to organized internal structure) and high viscosity of lyotropic phase. LLCs gel formulations can be a promise candidate for topical delivery of voriconazole, since the high viscosity of LLC phases and its more prolonged release profile may provide sustained skin concentrations of voriconazole for a prolonged time.

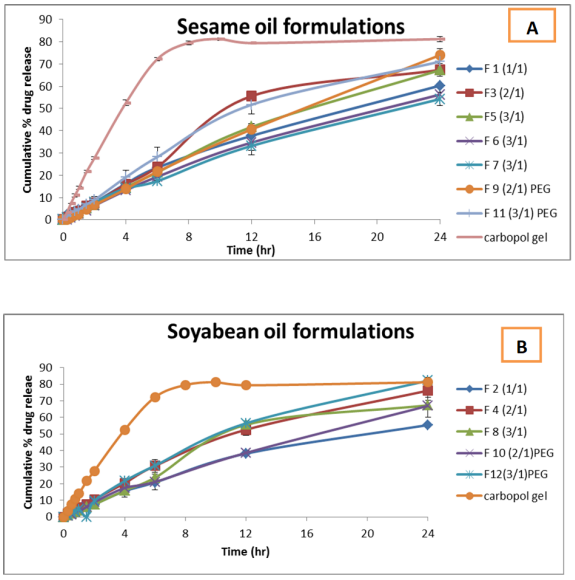

Fig. 5: *In-vitro* release profile of voriconazole from different LLC gel formulations based on: A. Sesame oil, B. Soyabean oil

These characteristics can improve patient compliance apart from reducing the frequency and severity of voriconazole side effects. LLC gel formulations containing PEG 600 as co-surfactant (F9, F11 and F12) have higher drug release % than LLC gel formulations containing glycerin as co-surfactant, this may be attributed to lower viscosity values of gel formulations containing PEG 600 as cosurfactant. This result was in agreement with the findings of Singh et al.[7], who found that release rate of metronidazole increased with lower viscosity of liquid crystalline systems. Another explanation is higher solubilization capacity of PEG 600 than glycerin, the equilibrium solubility of voriconazole in PEG 600 is (81.84 mg/mL) while in glycerin is (4.52 mg/mL), Prasanna et al.[6], reported that microemulsions with PEG 600 as cosurfactant had shown slightly enhanced voriconazole release compared to microemulsions which contain propylene glycol as cosurfactant at same S/Co ratios. El-Hadidy et al.[39]reported that prepared microemulsions using glycerol as the co-surfactant, showed significantly smaller voriconazole release values than MEs using sorbitol as co-surfactant, this retardant effect could be related to the higher viscosity of MEs contains glycerol. When comparing LLCs gel formulations containing the same components except for type of oil (F9 vs F10) and (F11 vs F12), it is clear that oil type has no significant effect on release rate of voriconazole. It may be attributed to that voriconazole has approximately same solubility in both two oils (equilibrium solubility of drug in sesame oil and soyabean oil is 7.37 mg/mL and 8.24 mg/mL respectively). As presented in Figure 6, The release of voriconazole from different LLC gel formulations after 24 hr can be ranked in the following descending order: (F12 > F4 > F9 > F11> F3, F5, F8 > F10 >

F1 > F6 > F2 > F7).

Mechanisms and kinetics of in-vitro drug release

Table 9 showed the results of fitted voriconazole release data from different LLC gel formulations to different kinetic models. The drug release from the gel formulations followed first order model except F9. The diffusion exponent (n) of Korsmeyer-peppas equation was > 0.89 which indicate super case II mechanism (swelling controlled).

Table 9: Kinetic analysis of *in-vitro* drug release data from different LLCs formulations

Formulation Code	Zero order (r^2)	First order (r^2)	Diffusion model (r^2)	Korsmeyer-Peppas (n)
F1	0.988476	**0.999337**	0.993693	0.910358
F2	0.981051	**0.995561**	0.995205	1.083683
F3	0.96322	**0.979823**	0.979726	1.047464
F4	0.980917	**0.999685**	0.994131	0.977313
F5	0.993117	**0.999398**	0.988042	1.010903
F6	0.991003	**0.999706**	0.992567	1.320652
F7	0.99244	**0.999384**	0.991379	0.91247
F8	0.96322	**0.979823**	0.979726	1.047464
F9	**0.998076**	0.993927	0.983536	1.427138
F10	0.994067	**0.997917**	0.990491	1.023487
F11	0.976819	**0.99674**	0.991957	0.910282
F12	0.977795	**0.998516**	0.988042	1.100592

Ex-vivo skin permeation study

Ex-vivo permeation of selected formulations F3, F4, F5 (Figure 6 **A**) F11 and F12 (Figure 6 **B**) were studied and carbopol gel containing 0.5 % w/w voriconazole was used as control. Figure 6 shows the cumulative amount permeated of voriconazole through skin from various formulations as function of time. It was found that significant ($p < 0.05$) increase in amount of voriconazole permeated from all LLC gel formulations compared to that permeated from carbopol gel (0.5 % w/w voriconazole). Several mechanisms have been proposed to explain the penetration-enhancing effect of LLC gel. Most likely, it is the overall combination of various mechanisms that result in the penetration-enhancing effect. The first possible mechanism was related to the similarity of LLC structures (lamellar and cubic phases) to the structure of skin. Liquid crystal-based formulation exhibits high hydration and easy distribution due to the similarity in the structures of LC and stratum corneum.

The cubic phase system exhibits strong bio-adhesive property and forms a biological membrane like structure over the skin on topical application [40,41]. Also, mesophases with a lamellar structure demonstrate great similarity to the intercellular lipid membrane of the skin [38]. The second possible mechanism is the penetration enhancing effect

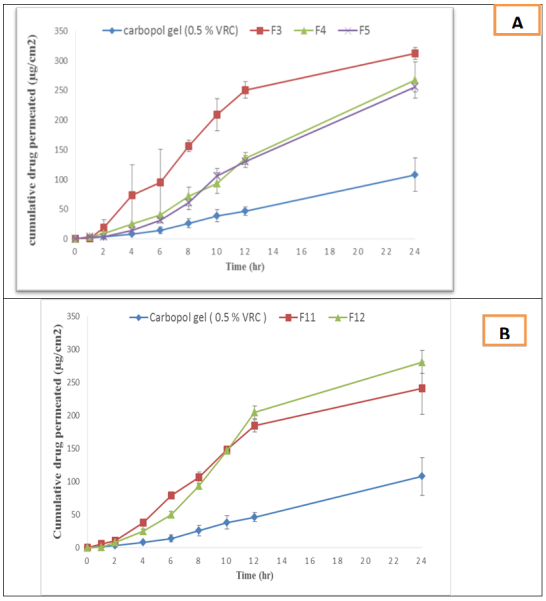

Fig. 6: *Ex-vivo* permeation profile of voriconazole from LLC gel formulations through rat skin

of LLC gel components. Through the use of a nonionic surfactant (Cremophor RH 40), a reversible increase in the permeability of the stratum corneum can be achieved without irreversible skin irritation. The LLC systems exhibit good penetration, due to the very low interfacial surface tension arising at the oil/water interface, and they may facilitate the progressive diffusion of biologically active substances into the skin or systemic circulation [38]. The third possible mechanism is the small nano oil droplets which provide a larger surface area for permeation of drug in to the skin [42].

When comparing LLCs gel formulations containing the same components except for type of oil (F11 vs F12), it's clear that oil type has no significant effect on skin permeation of voriconazole. It may be attributed to that drug has approximately same solubility in both two oils. Also, the results showed that formulation F3 containing S/Co ratio of 2:1 achieved a significant ($P< 0.05$) increase in skin permeation effect compared to formulation F5 containing S/Co ratio of 3:1. This may be attributed to higher viscosity of F5. This finding was not in accordance with results obtained by F4 which contain S/Co ratio of 2:1. The amount of voriconazole that permeate through skin (Q) was calculated and plotted against time. The slope of linear section of the figure was used to compute the transdermal drug flux (Jss) and the apparent permeability coefficient (Papp) was determined through Jss / Co equation where Co is the initial drug concentration [34] as shown in Table 10.

Table 10 showed that from all LLC gel formulations studied, formulations F3 and F12 provided fluxes higher

Table 10: *Ex-vivo* permeation parameters of voriconazole from LLC gel formulations through dorsal rat skin

Formulation	Flux ($\mu g.cm^{-2}.hr^{-1}$)	Papp x 10^{-3} ($cm.hr^{-1}$)
F3	14.75 ± 0.058	2.91
F4	11.55 ± 1.43	2.31
F5	11.28 ± 0.81	2.25
F11	11.17 ± 1.51	2.23
F12	13.13 ± 0.75	2.63
Carbopol gel (0.5% w/w voriconazole)	4.61 ± 1.13	0.92

than the rest of the formulations (F4, F5, F11). Also, F3 and F12exhibited higher permeability values for voriconazole. Both formulations (F3 and F12) were selected for further evaluation.

Skin deposition study

Skin deposition of the drug from different formulations was also investigated (Figure 7). The amount of drug deposited in skin from carbopol gel (0.5 % w/w voriconazole) was significantly lower than that from any of the LLC gel formulations ($p<0.05$). This enhanced skin deposition for the drug loaded into the LLC gel might be attributed to the enhanced penetration of the drug into the skin layers and structural similarity of the LLC structures with skin[43].

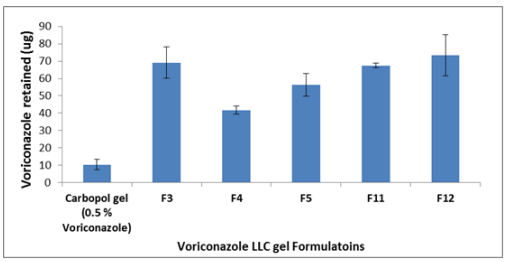

Fig. 7: *Ex-vivo* deposition of voriconazole in rat dorsal skin after 24 hr of application using different of LLC gel formulations

The amount of the drug deposited in skin after 24 hr was significantly higher ($P< 0.05$) for LLC gel formulations F3 and F12 when compared with F4, F5 and F11. So based on skin deposition and skin permeation results, F3 and F12 were selected for further evaluation.

Skin penetration behavior of LLC gel (CLSM imaging study)

Rhodamine B (log P: 1.95) was chosen as model compound which have similar lipophilic features with voriconazole (log P: 1.8) and loaded into optimized LLC gel formulations (F3 and F12) to visualize their penetration ability into skin layers[16]. The skin penetration enhancement effect of LLC and the localization of model fluorescent marker following the topical application of LLC gel formulation was visualized using CLSM.

The confocal images in Figure 8 showed that the LLC gel were able to deliver fluorescent dye to all skin layers at the end of 24 hr. These results were consistent with those of *in-vitro* skin permeation and deposition study. Taken together, CLSM images further confirm that LLC gel may significantly improve drug permeability and retention.

Rhodamine B dermal deposition concentrations are estimated based on fluorescent intensity in skin layers which were quantitatively analyzed by Image-J software[44]. As shown in Figure 8, the results obtained revealed that LLC formulations F3 and F12 Provide approximately the same Rhodamine B concentrations (fluorescence intensity) in all skin layers with no significant difference between the two formulations (F3 and F12).

The results suggest that the proposed formulations (F3 and F12) were able to deliver voriconazole up to and beyond the epidermis which can be suitable for topical fungal infection control. LLC gel formulation cause adherence to the stratum corneum followed by increased voriconazole penetration into viable layer of the skin (The extent of penetration into deeper skin layers at the depth up to 766 μm for F2 and up to 1079 μm for F12).

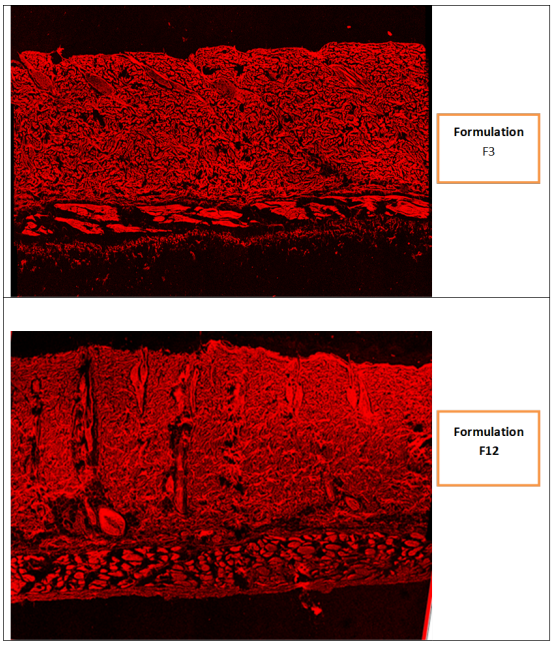

Fig. 8: Confocal laser scanning microscopy photograph of Dorsal rat skin treated with Rhodamine B – loaded LLC gel

Skin irritation study

Although all the materials used for preparation of LLC gel fell under the Generally Regarded as Safe (GRAS)

category, concentrations of all materials are a very critical issue for these formulations. For example, a large amount of surfactants is usually an irritant to the skin. Therefore, a skin irritation test was performed to confirm that the concentration of materials used for LLC gel preparation was safe. The results are shown in Table 11 and Figure 9. Draize et al.[45] mentioned that a value of the primary irritancy index (PII) < 2 indicates that the applied formulation is a non-irritant to human skin. Therefore, F12 and F3 were considered to be a non-irritant as PII was < 2. However, animals treated with 0.8% w/v aqueous formalin as standard irritant demonstrated PII = 6.43 ± 1.6 indicating high irritancy. Negative control group indicated no irritation as no medication was applied on to the skin. Therefore, on the basis of outcomes of this study, formulation can be declared as non-irritant and safe for skin application.

Table 11: Data of the skin irritation test

Day	Negative control		Formalin soln (0.8 % w/v)		F3		F12	
	ER	ED	ER	ED	ER	ED	ER	ED
1	0	0	2	3	0	0	0	0
2	0	0	3	4	0	0	0	0
3	0	0	3	4	0	0	0	1
4	0	0	4	3	0	0	0	0
5	0	0	4	2	1	0	1	0
6	0	0	4	2	0	0	0	0
7	0	0	4	3	0	0	0	0
Avg ± SD	0 ± 0	0 ± 0	3.43 ± 0.7	3 ± 0.82	0.14 ± 0.3	0 ± 0	0.14 ± 0.3	0.14 ± 0.3
PII	0 ± 0		6.43 ± 1.6		0.14 ± 0.37		0.28 ± 0.74	

ED = Edema, ER= Erythema, Avg= Average and PII= primary irritancy index

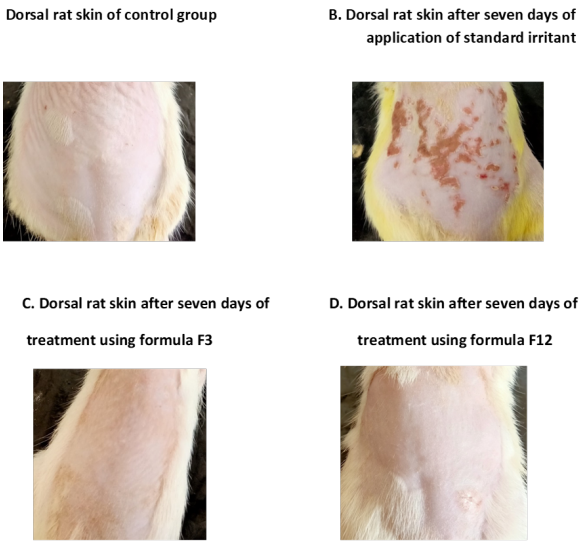

Fig. 9: Safety of the selected formulations (F3 & F12)

In-vitro antifungal activity

The agar diffusion method was performed to determine the effectiveness of the prepared LLC formulations with respect to carbopol gel (0.5 % w/w voriconazole) against different species of fungi including *Candida albicans, Aspergillus flavus* and *Aspergillus niger*. The antifungal activities were measured as diameter (mm) of zone of inhibition.

The results showed that the diameter of zone of inhibition obtained from LLC gel formulations (F3 and F12) was significantly higher than that of carbopol gel containing 0.5 %w/w voriconazole ($P<0.05$) while plain LLC gel formulations (F3 and F12) did not show any activity against all the examined strains of fungi as observed in Figure 10. These results indicating the superior antifungal activity efficacy of LLC gel formulations over carbopol gel containing 0.5 % w/w voriconazole. The enhanced *in-vitro* antifungal activity of LLC gel formulations may be attributed to enhanced penetration of oil globules containing voriconazole through fungal cell walls to inhibit ergosterol synthesis[46]. In addition, sustained release of voriconazole from LLC can control the growth of fungi for longer duration than carbopol gel (0.5 % w/w voriconazole)[2]. From Figure 10, it was clear that, the inhibition zone of voriconazole against *A. flavus* and *A. niger* was significantly higher than that of *C. albicans*. This was in agreement with the results obtained by Neslihan et al. who illustrated the significant activity of voriconazole against *Aspergillus* species[47].

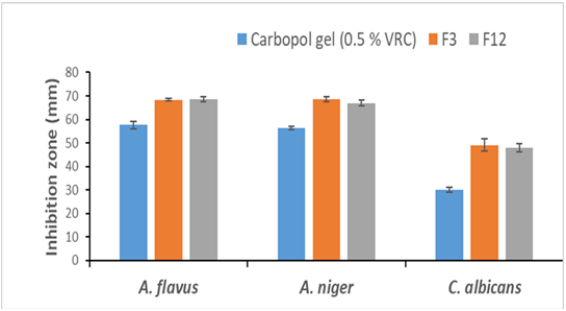

Fig. 10: The inhibition zone (mm) of F3, F12 and Carbopol voriconazole gel (0.5% w/w)

In-vivo antifungal study

- **Clinical investigations**

Evaluation of antifungal activity using *Candida albicans* is widely used. Before induction of superficial fungal infection,

all animals showed normal skin structure without any clinical features of fungal infection, for example inflammation, edema, cracking, or color changes[48]. After fungal infection induction, the animals were observed on daily basis for signs of infection. The topical treatment was started after 7 days, after the appearance of fungal infection signs (more intense redness, inflammation, scales, ulcers and edema) and confirmation of fungal infection on the skin of animals using light microscope (Figure 11). After continuous application of different treatments once daily for seven days: Negative control group showed normal skin without any sign of infection and no histological changes. On the other hand, positive control group presented slight decrease in skin elasticity with inflammation, ulcers and scares which confirmed by using histological image with necrosis and inflammatory cells infiltration in the dermis.

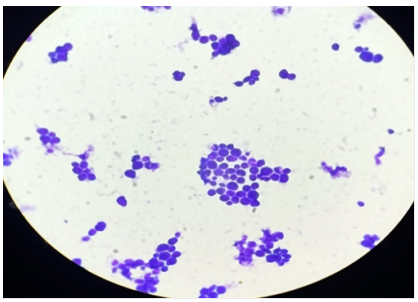

Fig. 11: Micrographic photo of *Candida albicans* under light microscope

In groups treated with LLC gel formulations (F3 and F12), fungal infection signs were significantly disappeared at day 5 and treatment was continued for another two days to ensure eradication of fungal infection as shown in Figure 12, while fungal infection signs (redness and inflammation and scales) were still present in groups treated with plain LLC formulations and carbopol gel (0.5 % w/w voriconazole).

The skin that had been treated with LLC gel (F3 and F12) seemed healthy and smooth, with no signs of infection like redness, swelling or scarring. These dramatic shifts suggest that LLC gel showed therapeutic effects on *Candida* skin infections, and these results were supported by histopathological examination.

Histopathology

Rats in negative control group had intact epidermis covered with normal keratin layer and dermis containing normally distributed skin adnexa (Figure 13**A**). Histopathological examination of skin from *Candida ablicans*-infected rats showed coagulation necrosis of sub-epidermal with formation of micro-abscesses at the dermis-epidermal junction (Figure 13**B**), hyperkeratosis and acanthosis (Figure 13 **C**). The dermis and subcutis revealed mononuclear cellular infiltration and loss of skin adnexa (Figure 13 **D**).

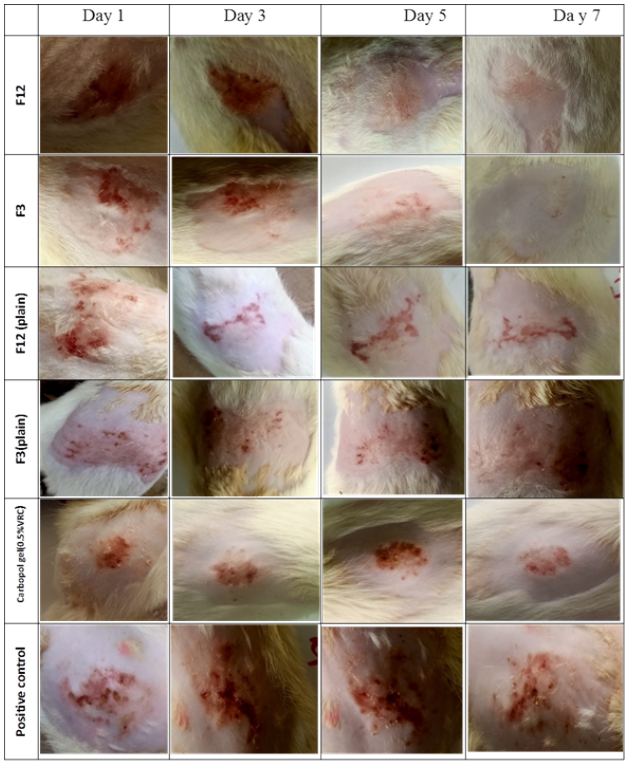

Fig. 12: Skin samples of different rats at days 1, 3, 5, and 7 of Treatment

On the other hand, treatment of *Candida ablicans*-infected skin with F12 formulation after 7 days of infection for 7 days resulted in formation of a thin epidermal layer covering the skin and absence of the mononuclear cellular infiltration in the dermis and subcutis (Figure 13 **C**). As well, treatment of *Candida ablicans*-infected rats with F3 formulation leads to formation of a well-developed epidermal layer on the skin and absence of the mononuclear cellular infiltration in the dermis and subcutis (Figure 13 **D**).

Similar treatment of infected rats with carbopol gel showed an improvement of skin histology except for denuded areas of epidermis alternated with areas of a canthosis and hyperkeratosis (Figure 13**G**).

Treatment of infected rats with either F12 plain or F3 plain caused no histological improvement in both epidermis and dermis. Animals showed loss of epidermal layer and degenerative changes of skin adnexa, and coagulation necrosis of sub-epidermal tissues (Figure 13**E** and **F**), respectively.

Stability study

The formulations were found to be stable for six months at room temperature and at 4-8 °C. Tables 12 and 13 show that, there was no change in appearance (color and turbidity), no phase separation, no drug precipitation. Also, there was no significant change in pH, drug content, and

Table 12: Stability study of the selected LLC gel formulations (F3 and F12) at room temperature

Parameters	Formulation	Sampling time (month)				
		6	3	2	1	Initial
Appearance	F3	No change	No change	No change	No change	Clear transparent
	F12	No change	No change	No change	No change	Clear transparent
pH	F3	5.7±0.23	6.13±0.12	6.21±0.18	6.20±0.26	6.21±0.1
	F12	5.6±0.15	5.8±0.1	5.86±0.05	5.87±0.03	5.9±0.096
Drug content (%w/w)	F3	97.31±2.0	98.20±1.42	99.24±2.66	97.17±2.95	98.65±1.11
	F12	98.65±3.36	98.35±2.7	98.20±1.6	98.8±1.53	100.1±1.7
Viscosity (mPa·s) X100000	F3	1.65 ±0.19	1.71± 0.14	1.56±0.34	1.8±0.021	1.93 ± 0.10
	F12	0.43±0.03	0.44±0.01	0.44±0.04	0.48±0.04	0.527±0.08
Droplet size (nm)	F3	25.06±2.5	**Not tested**			23.94± 1.5
	F12	35.78±1.6				23.70± 1.3
Zeta potential (mv)	F3	-3.01±0.25	**Not tested**			-7.35 ±0.1
	F12	-4.47±0.7				-7.46±0.5

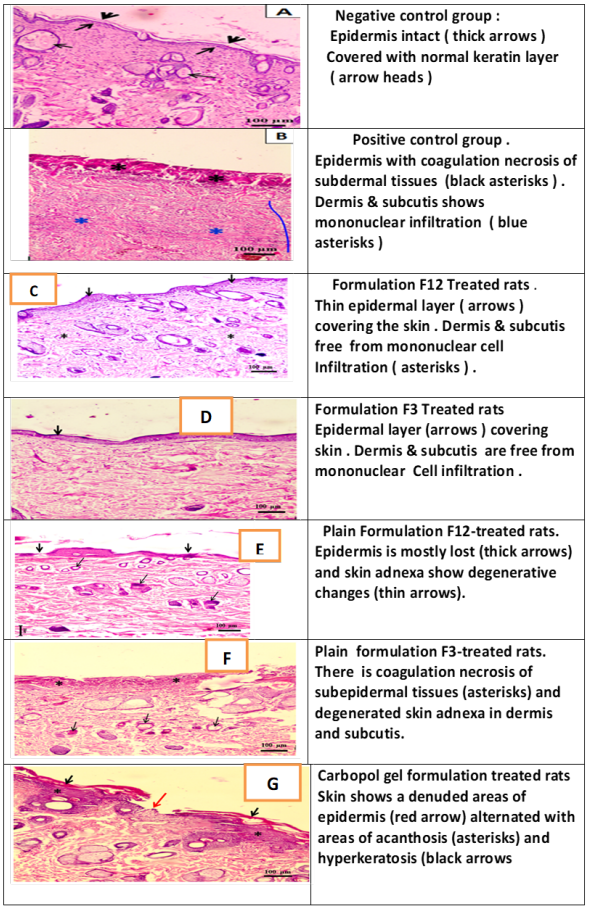

Fig. 13: Histopathological examination of rat skin infected by *Candida Ablicans* after seven days of Infection

viscosity. This was expected due to the thermodynamic stability of LLC gel system. However, other properties were slightly altered such as pH values of formulations (F3 and F12) as well as droplet size. The slight pH decrease of the two formulations may be attributed to greater number of hydrogen ion liberated from hydrolytic degradation of both oils (sesame and soyabean oils)[49]. On the other hand, the increase droplet size contributed to reduction in the zeta potential from -7.53 to -3.4 for F3 and from -7.46 to -4.47 for F12. Also, the reduction in zeta confirms liberation of hydrogen ion, which carry positive charge led to decrease negative charge (zeta potential) in the system.

CONCLUSIONS

Lyotropic liquid crystalline gel formulations (F3 and F12) are promising vehicle for topical delivery of voriconazole for treatment of skin fungal infections. Both formulations showed small nano droplet size 24.54 and 23.62 nm and zeta potential -13.7 and – 7.5 mv respectively, showed a sustained release pattern over 24 hours following first order mechanism. In permeability studies, both formulations had the highest flux and permeability coefficient compared to other formulations. *In-vitro* antifungal study showed that, both formulations had an excellent activity against different species of fungi. Furthermore, *in-vivo* studies showed that the developed formulations showed the superior antifungal activity on fungal skin infection induced by *Candida albicans*. Results of the skin irritation test indicated that F3 and F12 could be safe for human use.

Table 13: Stability of the selected LLC gel formulations (F3 and F12) at 4-8 ºC

Parameters	Formulation	Sampling time (month)				
		6	3	2	1	Initial
Appearance	F3	No change	No change	No change	No change	Clear transparent
	F12	No change	No change	No change	No change	Clear transparent
pH	F3	5.7±0.23	6.13±0.12	6.21±0.18	6.20±0.26	6.21±0.1
	F12	5.6±0.15	5.8±0.1	5.86±0.05	5.87±0.03	5.9±0.096
Drug content (%w/w)	F3	97.31±2.0	98.20±1.42	99.24±2.66	97.17±2.95	98.65±1.11
	F12	98.65±3.36	98.35±2.7	98.20±1.6	98.8±1.53	100.1±1.7
Viscosity (mPa·s) X100000	F3	1.65 ±0.19	1.71± 0.14	1.56±0.34	1.8±0.021	1.93 ± 0.10
	F12	0.43±0.03	0.44±0.01	0.44±0.04	0.48±0.04	0.527±0.08
Droplet size (nm)	F3	25.06±2.5	**Not tested**			23.94± 1.5
	F12	35.78±1.6				23.70± 1.3
Zeta potential (mv)	F3	-3.01±0.25	**Not tested**			-7.35 ±0.1
	F12	-4.47±0.7				-7.46±0.5

Acknowledgment

The authors would like to express their gratitude and appreciation to Prof. Dr. Sary Khaleel Abd Elghaffar Nasr faculty of Vetrinary Medicine, Pathology Department, Assiut University, Assiut, Egypt. For the interpretation of the Histopathological data.

- **Funding**

This research did not receive any specific grant from funding agencies in the public, commercial and not for profit sectors.

- **Author statement**

All authors made a significant contribution to the work reported, whether that is in the conception, study design, execution, acquisition of data, analysis and interpretation, or in all these areas; took part in drafting, revising or critically reviewing the article; gave final approval of the version to be published; have agreed on the journal to which the article has been submitted; and agree to be accountable for all aspects of the work.

- **Declaration of competing interest**

The authors declare that they have no known competing financial interests or personal relationships that have appeared to influence the work reported in this article.

REFERENCES

1. Gupta M, Sharma V, Chauhan NS. Nano- and Microscale Drug Delivery Systems. In: Promising novel nanopharmaceuticals for improving topical antifungal drug delivery,in Nano-and microscale drug delivery systems. Amsterdam, Netherlands. Elsevier. 2017;p. 197–228. Available from: https://doi.org/10.1016/B978-0-323-52727-9.00011-X.
2. Mumtaz T, Ahmed N, ul Hassan N, Badshah M, Khan S, ur Rehman A. Voriconazole nanoparticles-based film forming spray: An efficient approach for potential treatment of topical fungal infections. *Journal of Drug Delivery Science and Technology*. 2022;70. Available from: https://doi.org/10.1016/j.jddst.2021.102973.
3. Shah MKA, Azad AK, Nawaz A, Ullah S, Latif MS, Rahman H, et al. Formulation Development, Characterization and Antifungal Evaluation of Chitosan NPs for Topical Delivery of Voriconazole In Vitro and Ex Vivo. *Polymers*. 2022;14(1):1–17. Available from: https://doi.org/10.3390/polym14010135.
4. Liu W, Li M, Tian B, Yang X, Du W, Wang X, et al. Calcofluor white-cholesteryl hydrogen succinate conjugate mediated liposomes for enhanced targeted delivery of voriconazole into Candida albicans. *Biomaterials Science*. 2023;11(1):307–321. Available from: https://doi.org/10.1039/D2BM01263D.
5. Song SH, Lee KM, Kang JB, Lee SG, Kang MJ, Choi YW. Improved skin delivery of voriconazole with a nanostructured lipid carrier-based hydrogel formulation. *Chemical and Pharmaceutical Bulletin*. 2014;62(8):793–798. Available from: https://doi.org/10.1248/cpb.c14-00202.
6. Raju YP, Hyndavi N, Chowdary VH, Rajesh SN, Basha D, Tejeswari N. In vitro assessment of non-irritant microemulsified voriconazole hydrogel system. *Artificial Cells, Nanomedicine, and Biotechnology* . 2017;45(8):1539–1547. Available from: https://doi.org/10.1080/21691401.2016.1260579.
7. Singh VK, Pal K, Banerjee I, Pramanik K, Anis A, Al-Zahrani SM. Novel organogel based lyotropic liquid crystal physical gels for controlled delivery applications. *European polymer journal*. 2015;68:326–337. Available from: https://doi.org/10.1016/j.eurpolymj.2015.05.009.
8. Kumar R, Sinha VR. Preparation and optimization of voriconazole microemulsion for ocular delivery. *Colloids and Surfaces B: Biointerfaces*. 2014;117:82–88. Available from: https://doi.org/10.1016/j.colsurfb.2014.02.007.
9. Kim YH, Song CK, Jung E, Kim DH, Kim DD. A microemulsion-based hydrogel formulation containing voriconazole for topical skin delivery. *Journal of Pharmaceutical Investigation* . 2014;44(7):517–524. Available from: https://doi.org/10.1007/s40005-014-0159-7.
10. Morsi NM, Abdelbary GA, Ahmed MA. Silver sulfadiazine based cubosome hydrogels for topical treatment of burns: Development and in vitro/in vivo characterization. *European journal of pharmaceutics and biopharmaceutics*. 2014;86(2):178–189. Available from: https://doi.org/10.1016/j.ejpb.2013.04.018.
11. Benigni M, Pescina S, Grimaudo MA, Padula C, Santi P, Nicoli S. Development of microemulsions of suitable viscosity for cyclosporine skin delivery. *International journal of pharmaceutics*. 2018;545(1-2):197–205. Available from: https://doi.org/10.1016/j.ijpharm.2018.04.049.

12. Nikumbh KV, Sevankar SG, Patil MP. Formulation development, in vitro and in vivo evaluation of microemulsion-based gel loaded with ketoprofen. *Drug Delivery* . 2015;22(4):509–515. Available from: https://doi.org/10.3109/10717544.2013.859186.
13. Evelyn D, Chong C, Jaya RK, Muralidharan S, Dhanaraj SA, Kumar JR, et al. Development and evaluation of microemulsion based gel (mbgs) containing econazole nitrate for nail fungal infection. *Journal of Pharmacy Research*. 2012;5(4):2385–2390. Available from: https://www.researchgate.net/publication/230554563_Development_and_evaluation_of_microemulsion_based_gel_MBGs_containing_econazole_nitrate_for_nail_fungal_infection.
14. Abdulkarim MF, Abdullah GZ, Chitneni M, Salman IM, Ameer OZ, Yam MF, et al. Topical piroxicam in vitro release and in vivo anti-inflammatory and analgesic effects from palm oil esters-based nanocream. *International Journal of Nanomedicine*. 2010;5(1):915–924. Available from: https://doi.org/10.2147/IJN.S13305.
15. Safwat MA, Soliman GM, Sayed D, Attia MA. Gold nanoparticles capped with benzalkonium chloride and poly (ethylene imine) for enhanced loading and skin permeability of 5-fluorouracil. *Drug Development and Industrial Pharmacy*. 2017;43(11):1780–1791. Available from: https://doi.org/10.1080/03639045.2017.1339082.
16. Qurt MS, Esentürk İ, Tan SB, Erdal MS, Araman A, Güngör S. Voriconazole and sertaconazole loaded colloidal nano-carriers for enhanced skin deposition and improved topical fungal treatment. *Journal of Drug Delivery Science and Technology*. 2018;48:215–222. Available from: https://doi.org/10.1016/j.jddst.2018.09.020.
17. Guide for the care and use of laboratory animals;vol. 8. Washington, D.C.USA. National Academies Press. . Available from: https://grants.nih.gov/grants/olaw/guide-for-the-care-and-use-of-laboratory-animals.pdf.
18. Abdellatif MM, Khalil IA, Khalil MAF. Sertaconazole nitrate loaded nanovesicular systems for targeting skin fungal infection: In-vitro, ex-vivo and in-vivo evaluation. *International Journal of Pharmaceutics*. 2017;527(1-2):1–11. Available from: https://doi.org/10.1016/j.ijpharm.2017.05.029.
19. Al-Maghrabi PM, Khafagy ES, Ghorab MM, Gad S. Influence of formulation variables on miconazole nitrate-loaded lipid based nanocarrier for topical delivery. *Colloids and Surfaces B: Biointerfaces*. 2020;193. Available from: https://doi.org/10.1016/j.colsurfb.2020.111046.
20. Guo F, Wang J, Ma M, Tan F, Li N. Skin targeted lipid vesicles as novel nano-carrier of ketoconazole: characterization, in vitro and in vivo evaluation. *Journal of Materials Science: Materials in Medicine*. 2015;26(4):1–13. Available from: https://doi.org/10.1007/s10856-015-5487-2.
21. Moretti A, Boncio L, Posteraro B, Mechelli L, Balducci M, Fadda G, et al. Co-cutaneous infection in a dog: PCR-reverse identification of Candida tropicalis on skin biopsy. *Journal de Mycologie Médicale*. 2006;16(1):30–36. Available from: https://doi.org/10.1016/j.mycmed.2006.01.004.
22. Mei L, Xie Y, Huang Y, Wang B, Chen J, Quan G, et al. Injectable in situ forming gel based on lyotropic liquid crystal for persistent postoperative analgesia. *Acta Biomaterialia*. 2018;67:99–110. Available from: https://dx.doi.org/10.1016/j.actbio.2017.11.057.
23. Khare A, Singh I, Pawar P, Grover K. Design and evaluation of voriconazole loaded solid lipid nanoparticles for ophthalmic application. *Journal of drug delivery*. 2016;2016:1–11. Available from: https://doi.org/10.1155/2016/6590361.
24. Helmy SA, El-Bedaiwy HM, El-Masry SM. Applying Biopharmaceutical Classification System criteria to predict the potential effect of Cremophor® RH 40 on fexofenadine bioavailability at higher doses. *Therapeutic Delivery*. 2020;11(7):447–464. Available from: https://dx.doi.org/10.4155/tde-2020-0042.
25. Petrović ZS. Polyurethanes from Vegetable Oils. *Polymer Reviews*. 2008;48(1):109–155. Available from: https://www.tandfonline.com/doi/abs/10.1080/15583720701834224.
26. Mirghani MES, Man YBC, Jinap S, Baharin BS, Bakar J. Application of FTIR spectroscopy in determining sesamol in sesame seed oil. *Journal of the American Oil Chemists' Society*. 2003;80(1):1–4. Available from: https://dx.doi.org/10.1007/s11746-003-0640-1.
27. Ahmed MK, McLeod MP, Nézivar J, Giuliani AW. Fourier transform infrared and near-infrared spectroscopic methods for the detection of toxic Diethylene Glycol (DEG) contaminant in glycerin based cough syrup. *Journal of Spectroscopy*. 2010;24(6):601–608. Available from: https://dx.doi.org/10.1155/2010/608749.
28. Thakur A, Tripathi M, Rajesh UC, Rawat DS. Ethylenediammonium diformate (EDDF) in PEG600: an efficient ambiphilic novel catalytic system for the one-pot synthesis of 4H-pyrans via Knoevenagel condensation. *RSC Advances*. 2013;3(39):18142–18142. Available from: https://dx.doi.org/10.1039/c3ra42410c.
29. Cardoso CO, Ferreira-Nunes R, Cunha-Filho M, Gratieri T, Gelfuso GM. In situ gelling microemulsion for topical ocular delivery of moxifloxacin and betamethasone. *Journal of Molecular Liquids*. 2022;360. Available from: https://dx.doi.org/10.1016/j.molliq.2022.119559.
30. Moreno MA, Ballesteros MP, Frutos P. Lecithin-based oil-in-water microemulsions for parenteral use: Pseudoternary phase diagrams, characterization and toxicity studies. *Journal of Pharmaceutical Sciences*. 2003;92(7):1428–1437. Available from: https://dx.doi.org/10.1002/jps.10412.
31. Kale NJ, Jr LVA. Studies on microemulsions using Brij 96 as surfactant and glycerin, ethylene glycol and propylene glycol as cosurfactants. *International Journal of Pharmaceutics*. 1989;57(2):87–93. Available from: https://dx.doi.org/10.1016/0378-5173(89)90296-2.
32. Patel RB, Patel MR, Bhatt KK, Patel BG. Formulation consideration and characterization of microemulsion drug delivery system for transnasal administration of carbamazepine. *Bulletin of Faculty of Pharmacy, Cairo University*. 2013;51(2):243–253. Available from: https://doi.org/10.1016/j.bfopcu.2013.07.002.
33. Bikkad ML, Nathani AH, Mandlik SK, Shrotriya SN, Ranpise NS. Halobetasol propionate-loaded solid lipid nanoparticles (sln) for skin targeting by topical delivery. *Journal of Liposome Research* . 2014;24(2):113–123. Available from: https://doi.org/10.3109/08982104.2013.843192.
34. Shewaiter MA, Hammady TM, El-Gindy A, Hammadi SH, Gad S. Formulation and characterization of leflunomide/diclofenac sodium microemulsion base-gel for the transdermal treatment of inflammatory joint diseases. *Journal of Drug Delivery Science and Technology*. 2021;61. Available from: https://doi.org/10.1016/j.jddst.2020.102110.
35. Patel P, Pol A, Kalaria D, Date AA, Kalia Y, Patravale V. Microemulsion-based gel for the transdermal delivery of rasagiline mesylate: In vitro and in vivo assessment for parkinson's therapy. *European Journal of Pharmaceutics and Biopharmaceutics*. 2021;165:66–74. Available from: https://doi.org/10.1016/j.ejpb.2021.04.026.
36. Savic S, Pantelic I, Lukic M, Markovic B, Milic J. Behind the Alkyl Polyglucoside-based structures: Lamellar liquid crystalline and lamellar gel phases in different emulsion systems. In: Alkyl Polyglucosides. Elsevier. 2014;p. 21–52. Available from: https://doi.org/10.1533/9781908818775.21.
37. Li Q, Cao J, Li Z, Chu X. Cubic Liquid Crystalline Gels Based on Glycerol Monooleate for Intra-articular Injection. *AAPS PharmSciTech*. 2018;19:858–865. Available from: https://doi.org/10.1208/s12249-017-0894-y.
38. Makai M, Csányi E, Németh Z, Palinkas J, Erős I. Structure and drug release of lamellar liquid crystals containing glycerol. *International Journal of Pharmaceutics*. 2003;256(1-2):95–107. Available from: https://doi.org/10.1016/S0378-5173(03)00066-8.
39. El-Hadidy GN, Ibrahim HK, Mohamed MI, El-Milligi MF. Microemulsions as vehicles for topical administration of voriconazole: formulation and in vitro evaluation. *Drug Development and Industrial Pharmacy*. 2012;38(1):64–72. Available from: https://doi.org/10.3109/03639045.2011.590731.
40. Rapalli VK, Waghule T, Hans N, Mahmood A, Gorantla S, Dubey SK, et al. Insights of lyotropic liquid crystals in topical drug delivery for targeting various skin disorders. *Journal of molecular liquids*. 2020;315. Available from: https://doi.org/10.1016/j.molliq.2020.113771.

41. Luo M, Shen Q, Chen J. Transdermal delivery of paeonol using cubic gel and microemulsion gel. *International Journal of Nanomedicine*. 2011;6:1603–1610. Available from: https://doi.org/10.2147/IJN.S22667.
42. Elmataeeshy ME, Sokar MS, Bahey-El-Din M, Shaker DS. Enhanced transdermal permeability of terbinafine through novel nanoemulgel formulation; development, in vitro and in vivo characterization. *Future journal of pharmaceutical sciences*. 2018;4(1):18–28. Available from: https://doi.org/10.1016/j.fjps.2017.07.003.
43. Mazzotta E, Rossi CO, Muzzalupo R. Different BRIJ97 colloid systems as potential enhancers of acyclovir skin permeation and depot. *Colloids and Surfaces B: Biointerfaces*. 2019;173:623–631. Available from: https://doi.org/10.1016/j.colsurfb.2018.10.041.
44. Zhang J, Michniak-Kohn BB. Investigation of microemulsion and microemulsion gel formulations for dermal delivery of clotrimazole. *International Journal of Pharmaceutics*. 2018;536(1):345–352. Available from: https://doi.org/10.1016/j.ijpharm.2017.11.041.
45. Draize JH, Woodard G, Calvery HO. Methods for the study of irritation and toxicity of substances applied topically to the skin and mucous membranes. *Journal of Pharmacology and Experimental Therapeutics*. 1944;82(3):377–390. Available from: https://jpet.aspetjournals.org/content/82/3/377.
46. Bachhav YG, Patravale VB. Microemulsion based vaginal gel of fluconazole: Formulation, in vitro and in vivo evaluation. *International Journal of Pharmaceutics*. 2009;365(1-2):175–179. Available from: https://doi.org/10.1016/j.ijpharm.2008.08.021.
47. Okur NÜ, Yozgatlı V, Okur ME, Yoltaş A, Siafaka PI. Improving therapeutic efficacy of voriconazole against fungal keratitis: Thermosensitive in situ gels as ophthalmic drug carriers. *Journal of Drug Delivery Science and Technology*. 2019;49:323–333. Available from: https://doi.org/10.1016/j.jddst.2018.12.005.
48. Qushawy M, Nasr A, Abd-Alhaseeb M, Swidan S. Design, optimization and characterization of a transfersomal gel using miconazole nitrate for the treatment of candida skin infections. *Pharmaceutics*. 2018;10(1):1–22. Available from: https://doi.org/10.3390/pharmaceutics10010026.
49. Pajic NB, Nikolic I, Mitsou E, Papadimitriou V, Xenakis A, Randjelovic D, et al. Biocompatible microemulsions for improved dermal delivery of sertaconazole nitrate: Phase behavior study and microstructure influence on drug biopharamaceutical properties. *Journal of molecular liquids*. 2018;272:746–758. Available from: https://doi.org/10.1016/j.molliq.2018.10.002.